Mechanics of Advanced Composite Structures 9 (2022) 229 – 242

Semnan University

Mechanics of Advanced Composite Structures

journal homepage: http://MACS.journals.semnan.ac.ir

Nonlinear Torsional Vibration Analysis of Nanorods in the Presence of Surface Energy Effect: Multi-Mode Galerkin Method

R. Nazemnezhad*, S. Farahmandrad

School of Engineering, Damghan University, Damghan, Iran

KEYWORDS

Nonlinear torsional vibration;
Multiple-scale method;
Internal resonances;
Multi-mode Galerkin method;
Surface energy.

ABSTRACT

In this paper, the nonlinear torsional vibrations and internal resonances of nanorods are investigated by considering the surface energy effects. For this purpose, Hamilton's principle is implemented to derive the nonlinear governing equation of motion based on the von-Kármán relations. Hamilton's principle includes the strain energy and the kinetic energy of the nanorod surface and bulk. The strain and kinetic energies of the nanorod bulk are obtained using the classical theory of elasticity, and those of the nanorod surface are obtained using the surface elasticity theory. The surface energy parameters, including the surface density and the surface Lame constants, are included in the equations by the surface elasticity theory. Then, the multi-mode Galerkin method is used to convert the partial differential equation of motion to an ordinary differential equation. The Multiple-scale method is employed to solve the governing equations of motion for fixed-free and fixed-fixed end conditions. To investigate the technique presented in this paper, circular nanorods made of aluminum and silicon have been used. The effect of surface energy parameters on the torsional frequencies of nanorods is investigated for different values of length, radius, frequency number, and amplitude of the nonlinear vibrations. In addition, the cases in which internal resonances occur are reported, and some numerical data are given. The results obtained in this research may be helpful for the better design of nanoelectromechanical devices such as nano-bearings and rotary servo motors.

1. Introduction

These days, nanostructures have captured significant attention due to their excellent physical and mechanical performance, surface stress, and size effects [1-6]. At the macroscale, since surface energy is small compared to the bulk energy, the effect of surface energy is not considered. Because the ratio of surface/volume in nano-scaled structures is high, the surface effects become important. Therefore, surface energy has a critical role in the mechanical analysis of nanostructures and should be considered. The classical continuum mechanics are not size-dependent, and consequently, several new continuum mechanics theories are necessary for analyzing nano-scaled structures. To investigate the effect of surface stress on the mechanics of nanostructures, Gurtin et al. [7, 8] introduced a mathematical theory for the exact prediction of mechanical behaviors of nano-scaled structures. Consequently, the number of studies reported in this field increased rapidly, especially in recent years.

A continuum model for nanobeams, including both surface effects and material heterogeneity, was developed by Baron et al. [9]. Wang and Feng presented a theoretical model directed toward investigating the effects of both surface elasticity and residual surface tension on the natural frequency of microbeams [10]. Ansari and Sahmani [11] studied the bending and buckling of nanobeams by using the Gurtin and Murdoch theory. They derived explicit formulas for different beam theories. Ansari et al. [12] developed a modified continuum model to predict the post-buckling deflection of nanobeams incorporating the effect of surface stress. They used the generalized differential quadrature (GDQ) method to solve governing differential equations. A comprehensive model was presented by Abbasion et al. [13] to investigate the influence of surface elasticity and residual surface tension on the natural frequency

* Corresponding author. Tel./Fax: +98-23-35220414.
E-mail addresses: rnazemnezhad@du.ac.ir; mrnazemnezhad@gmail.com

DOI: 10.22075/macs.2022.24331.1360
Received 2021-09-24; Received in revised form 2022-05-02; Accepted 2022-07-31

of flexural vibrations of microbeams in the presence of rotary inertia and shear deformation effects. An analytical model for predicting surface effects on the free vibration of fluid-conveying nanotubes based on the nonlocal elasticity theory was developed by Wang [14]. The results demonstrated that the surface effects with positive elastic constant or positive residual surface tension tend to raise the natural frequency and critical flow velocity. Farshi et al. [15] modified the Timoshenko beam model to study the surface effects and used it to analyze the vibration of nanotubes as well as calculate their natural frequencies. He and Lilley [16] studied the effect of surface stress and surface elasticity on the elastic behavior of nanowires in static bending. They used the Euler–Bernoulli beam theory and considered three different boundary conditions: cantilever, simply supported, and fixed–fixed. Fang et al. [17] investigated the size-dependent vibration of nano-sized piezoelectric double-shell structures under simply-supported boundary condition by combining Goldenveizer-Novozhilov shell theory, thin plate theory, and electro-elastic surface theory.

Recently, some studies have been performed to study the surface effects on the nonlinear free vibration behaviors of nanobeams. Nazemnezhad et al. [18] investigated the nonlinear free vibration of nanobeams with considering surface effects using Euler–Bernoulli beam theory. Based on the Gurtin-Murdoch continuum theory, Ansari et al. [19] studied the nonlinear free vibration behavior of Timoshenko nanobeams subject to different end conditions. Asgharifard Sharabiani et al. [20] analyzed the nonlinear free vibration of functionally graded Euler-Bernoulli nanobeams. In another work, Zhu et al. [21] considered the surface energy effect on nonlinear free vibration of viscoelastic orthotropic piezoelectric doubly-curved smart nanoshells by a new approach. In addition, Zhu et al. [22] investigated the surface energy effect on the nonlinear free vibration behavior of orthotropic piezoelectric cylindrical nano-shells by introducing an electro-elastic surface/interface model.

When nanotubes are subjected to the external torques, the torsional vibration becomes vital in some devices such as nanoelectromechanical systems, nano-scaled shafts, and nanoservomotors. There are not many studies about the free torsional vibration of nanotubes. Lim et al. [23] developed a new elastic nonlocal stress model and analytical solutions for torsional dynamic behaviors of circular nanorods/nanotubes. They investigated the free torsional vibration of nanorods/nanotubes and axially moving nanorods/nanotubes. Li and Hi [24] studied the free torsional vibration behaviors of nanotubes made of a bi-directional functionally graded (FG) material in which the material properties vary continuously along with the radius and length directions. Based on Nonlocal elasticity, Murmu et al. [25] analyzed the torsional vibration of single-walled carbon nanotube–buckyball systems. The buckyball was attached to a single-walled carbon nanotube (SWCNT) at one end, and the other end of the SWCNT was fixed. Torsional vibration analysis of nanobeams with a peripheral crack and different end conditions was investigated by Nazemnezhad and Fahimi [26]. They considered surface energy effects, including the surface stress, the surface shear modulus, and the surface density, on the torsional vibration of nanobeams with various boundary conditions. The stability of different types of single-walled carbon nanotubes (SWCNTs), rested in Winkler elastic foundations by considering the surface energy and surface residual stresses, was studied by Jena et al. [27,28]. Malikan et al. [29] analyzed the torsional buckling of a nano-composite shell employing first-order shear deformation shell theory. With the help of the finite element method, the nonlinear vibrational characteristics of a hetero-nanotube in the magneto-thermal environment were investigated by Sedighi and Malikan [30]. Sedighi et al. [31] used nonlinear finite element formulation to deal with the nonlocal vibrational behavior of carbon/boron-nitride nano-hetero-tubes in the presence of a magneto-thermal environment. Nonlinear free vibration of nanotubes under a magnetic environment was studied by Malikan and Eremeyev [32]. The magnetic force is applied to the conductive nanotube with a piezo-flexomagnetic elastic wall. The Euler-Bernoulli beam theory was conducted to extract governing equations of motion. In another work, Zarezadeh et al. [33] studied the size effects in FG nano-rod under a magnetic field supported by a torsional foundation based on the nonlocal elasticity. In this work, torsional vibration behavior was analyzed. Based on the nonlocal strain gradient elasticity, torsional vibration analysis of bi-directional FG nonlinear nano-cones with arbitrary cross-section was investigated by Noroozi et al. [34]. In another similar work, static torsion of bi-directional functionally graded microtube was analyzed based on the couple stress theory under magnetic field by Barati et al. [35].

According to the best author's knowledge, surface effects on the nonlinear torsional vibration of nanorods have not been considered yet. Therefore, the aims of the present study are 1) modeling the nonlinear torsional vibration of nanorods by considering the surface energy effects, 2) using the multi-mode Galerkin method

for converting the partial differential equation to an ordinary differential equation, 3) extracting and reporting the conditions in which the internal resonances occur.

In this paper, the nonlinear torsional vibration of nanorods considering the effect of various parameters such as nanorod dimensions, boundary conditions, and frequency number on natural nonlinear torsional frequencies of the nanorod is studied. Hamilton's principle is used to derive the equation of motion, and the multiple scale method is used to solve these equations.

2. Governing Equations

We consider a nanorod with length L and diameter D, as shown in Fig. 1. According to Fig. 1, the coordinate origin is chosen on the left side, and the area of the nanorod's cross-section is in the xy plane. The displacement components for torsion of the rod (U_x, U_y, U_z) are given as [36,37]

$$U_x = 0 \tag{1}$$

$$U_y = -z\theta(x,t) \tag{2}$$

$$U_z = y\theta(x,t) \tag{3}$$

where $\theta(x,t)$ donates angular displacement about the center of twist and t is time.

Based on von-Kármán theory, the geometrically nonlinear strain–displacement relations can be expressed as following [38,39]

$$\varepsilon_{xx} = \frac{1}{2}(y^2+z^2)\left(\frac{\partial\theta}{\partial x}\right)^2; \qquad \varepsilon_{yy} = \frac{1}{2}\theta^2$$

$$\varepsilon_{xz} = \frac{1}{2}\left(y\frac{\partial\theta}{\partial x} + z\theta\frac{\partial\theta}{\partial x}\right); \qquad \varepsilon_{yz} = 0 \tag{4}$$

$$\varepsilon_{xy} = \frac{1}{2}\left(-z\frac{\partial\theta}{\partial x} + y\theta\frac{\partial\theta}{\partial x}\right); \qquad \varepsilon_{zz} = \frac{1}{2}\theta^2$$

Based on linearized elasticity, the stress components are given by [38,39]

$$\begin{aligned}
\sigma_{xx} &= G_3\left[(1-\nu)\left(\frac{1}{2}\right)(y^2+z^2)\left(\frac{\partial\theta}{\partial x}\right)^2 + \nu(\theta^2)\right]\\
\sigma_{yy} &= G_3\left[\nu\left(\frac{1}{2}\right)(y^2+z^2)\left(\frac{\partial\theta}{\partial x}\right)^2 + \left(\frac{1}{2}\theta^2\right)\right]\\
\sigma_{zz} &= G_3\left[\nu\left(\frac{1}{2}\right)(y^2+z^2)\left(\frac{\partial\theta}{\partial x}\right)^2 + \left(\frac{1}{2}\theta^2\right)\right]\\
\sigma_{xy} &= G_3\left[\left(\frac{1-2\nu}{2}\right)\left(-z\frac{\partial\theta}{\partial x} + \frac{1}{2}y\theta\frac{\partial\theta}{\partial x}\right)\right]\\
\sigma_{xz} &= G_3\left[\left(\frac{1-2\nu}{2}\right)\left(y\frac{\partial\theta}{\partial x} + \frac{1}{2}z\theta\frac{\partial\theta}{\partial x}\right)\right]\\
\sigma_{yz} &= 0.
\end{aligned} \tag{5}$$

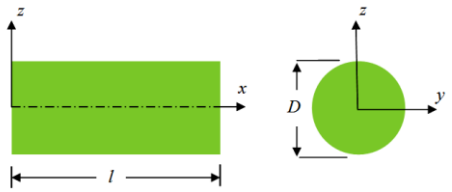

Fig. 1. Geometry of nanorod

To get the surface stresses, it should be noted that due to the high surface-to-volume ratio, nanoscale elements usually exhibit a great influence of surface/interface free energy, which is the energy associated with atoms at or near a free surface; consequently, their mechanical behavior becomes size-dependent. Thus, surface energy effects, which are generally ignored in conventional continuum mechanics problems, need to be considered in modified continuum-based simulation for nanoscale systems. A theoretical framework based on continuum mechanics concepts was proposed by Gurtin and Murdoch [7,8] to take into consideration the influence of surface energy effects. According to Gurtin and Murdoch, the surface district of a solid can be modeled as a layer of disappearing thickness sticking to the solid without sliding. For an isotropic, linear elastic material, the usual equations for the static elastic field in the inside of the solid are explained as

$$\begin{aligned}
&\nabla.\boldsymbol{\sigma} = 0\\
&\boldsymbol{\sigma} = 2\mu\boldsymbol{\varepsilon} + \lambda(tr\varepsilon)\boldsymbol{I}\\
&\boldsymbol{\varepsilon} = \frac{1}{2}[\Delta u + (\Delta u)^T]
\end{aligned} \tag{6}$$

where σ, ε, and u are stress, strain, and displacement components, respectively, μ and λ denote Lamé constants, and I is the unity tensor. They presented the constitutive equations of the surface stresses as follows

$$\begin{aligned}
\overline{\sigma}_{ij} &= \overline{\sigma}_0\,\delta_{ij} + 2\left(\overline{\mu} - \overline{\sigma}_0\right)\varepsilon_{ij}\\
&\quad + \left(\overline{\lambda} + \overline{\sigma}_0\right)u_{k,k}\delta_{ij} + \overline{\sigma}_0 u_{ij}
\end{aligned} \tag{7}$$

where $\overline{\sigma}_0$, $\overline{\lambda}$ and $\overline{\mu}$ are the surface residual stress under unstrained conditions, and surface Lamé parameters, respectively; u_i and δ_{ij} are the displacement components of the surfaces and Kronecker delta, respectively. The parameters with bar symbols belong to surface properties.

Substituting Eqs. (1)-(4) into Eq. (7) results in the surface stress components as

$$\begin{aligned}
&\overline{\sigma}_{xx} = \overline{\mu}(y^2+z^2)\left(\frac{\partial\theta}{\partial x}\right)^2;\\
&\bar{\sigma}_{yy} = \overline{\mu}\theta^2;\\
&\bar{\sigma}_{zz} = \overline{\mu}\theta^2;\\
&\bar{\sigma}_{xy} = 2\overline{\mu}\left[-z\frac{\partial\theta}{\partial x} + \frac{1}{2}y\theta\frac{\partial\theta}{\partial x}\right];\\
&\bar{\sigma}_{xz} = 2\overline{\mu}\left[y\frac{\partial\theta}{\partial x} + \frac{1}{2}z\theta\frac{\partial\theta}{\partial x}\right];\\
&\bar{\sigma}_{yz} = 0.
\end{aligned} \tag{8}$$

Hamilton's principle is implemented to obtain the equations for torsional vibration of nanorod based on the surface effect theory:

$$\delta \int_{t_1}^{t_2} (U - T - K)dt = 0 \tag{9}$$

where U, T, and K are the strain energy, the kinetic energy, and the work done by external forces, respectively. After applying Hamilton's principle, the governing equation of motion for torsional vibration of nanorod is obtained as follows

$$\begin{aligned} &\left(-\frac{3}{2}G_1 I_{P_2} - 3\overline{\mu}A_1\right)\left(\frac{\partial\theta}{\partial x}\right)^2\left(\frac{\partial^2\theta}{\partial x^2}\right) + \\ &(G_3 A + 2\overline{\mu}S)\theta^3 - \left(GI_{P_1} + 2A_2\overline{\mu}\right)\frac{\partial^2\theta}{\partial x^2} - \\ &\left(G_2 I_{P_1} + \frac{GI_{P_1}}{4} + \frac{A_2\overline{\mu}}{2}\right)\theta\left(\frac{\partial\theta}{\partial x}\right)^2 - \\ &\left(G_2 I_{P_1} + \frac{GI_{P_1}}{4} + \frac{A_2\overline{\mu}}{2}\right)\theta^2\left(\frac{\partial^2\theta}{\partial x^2}\right) \\ &\qquad - \left(+\rho I_{P_1} + A_2\bar{\rho}\right)\frac{\partial^2\theta}{\partial t^2} \\ &\qquad = 0 \end{aligned} \tag{10}$$

where

$$\begin{aligned} &G = \tfrac{E}{2(1+\nu)}; \quad G_1 = \tfrac{E(1-\nu)}{(1+\nu)(1-2\nu)}; \\ &G_2 = \tfrac{E\nu}{2(1+\nu)}; \quad G_3 = \tfrac{E}{(1+\nu)(1-2\nu)}; \\ &\left\{I_{P_1}, I_{P_2}\right\} = \int (y^2 + z^2)^{1,2} dA\,; \\ &\{A_1, A_2\} = \int (y^2 + z^2)^{1,2} ds\,;\ A = \pi R^2; \end{aligned} \tag{11}$$

We can rewrite Eq. (10) as follow

$$\begin{aligned} &\alpha_1\left(\frac{\partial\theta}{\partial x}\right)^2\frac{\partial^2\theta}{\partial x^2} + \alpha_2\theta^3 + \alpha_3\frac{\partial^2\theta}{\partial x^2} \\ &\qquad + \alpha_4\left(\theta\left(\frac{\partial\theta}{\partial x}\right)^2\right. \\ &\qquad \left. + \theta^2\frac{\partial^2\theta}{\partial x^2}\right) + \alpha_5\frac{\partial^2\theta}{\partial t^2} \\ &\qquad = 0 \end{aligned} \tag{12}$$

where in Eq. (12)

$$\begin{aligned} &\alpha_1 = -\frac{3}{2}G_1 I_{P_2} - 3\overline{\mu}A_1; \\ &\alpha_2 = G_3 A + 2\overline{\mu}S; \alpha_3 = -GI_{P_1} - 2A_2\overline{\mu}; \\ &\alpha_4 = -G_2 I_{P_1} - \frac{1}{4}GI_{P_1} - \frac{1}{2}A_2\overline{\mu}; \\ &\alpha_5 = -\rho I_{P_1} - A_2\bar{\rho}. \end{aligned} \tag{13}$$

The equation of spatial function and the boundary conditions are obtained by ignoring the nonlinear parameters in Eq. (12)

$$\alpha_3\frac{\partial^2\theta}{\partial x^2} + \alpha_5\frac{\partial^2\theta}{\partial t^2} = 0 \tag{14}$$

$$\left[\alpha_1\frac{\partial^2\theta}{\partial x^2}\right]\delta\theta\Big|_0^l = 0 \tag{15}$$

The separation-of-variables method is used to solve Eq. (14) and find the natural frequencies of nanorod

$$\theta(x,t) = \phi(x)e^{-i\omega_L t} \tag{16}$$

where ω_L is the linear torsional natural frequency. Substituting Eq. (16) into Eq. (14) and (15) yields the following equations

$$\alpha_3\frac{d^2\phi}{dx^2} - \alpha_5{\omega_L}^2 = 0 \tag{17}$$

$$\left[\alpha_1\frac{d^2\phi}{dx^2}\right]\delta\phi\Big|_0^l = 0 \tag{18}$$

By solving Eq. (17), we have

$$\phi(x) = C_1 Sin(\beta x) + C_2 Cos(\beta x) \tag{19}$$

where $\beta = \sqrt{\frac{\alpha_5}{\alpha_1}{\omega_L}^2}$. To obtain natural frequencies and mode shapes of nanorod we apply boundary conditions, Eq. (18), to Eq. (19). The mode shapes and natural frequencies of nanorod with fixed–fixed and fixed-free boundary conditions are expressed as

- Fixed-Fixed

$$\phi_n(x) = C_1 Sin\left(\frac{n\pi}{L}x\right) \tag{20}$$

$$\omega_L)_n = \left(\frac{n\pi}{L}\right)\sqrt{\frac{\alpha_5}{\alpha_1}} \tag{21}$$

- Fixed-Free

$$\phi_n(x) = C_1 Sin\left(\frac{(2n-1)\pi}{2L}x\right) \tag{22}$$

$$\omega_L)_n = \left(\frac{(2n-1)\pi}{2L}\right)\sqrt{\frac{\alpha_5}{\alpha_1}} \tag{23}$$

To convert the partial differential equation (Eq. (12)) to an ordinary differential equation, there are two choices:

- Single-mode Galerkin method

$$\theta(x,t) = \phi(x)\,q(t) \tag{24}$$

- Multi-mode Galerkin method

$$\theta(x,t) = \sum_{i=1}^{\square}\phi_i(x)\,q_i(t) \tag{25}$$

where $q(t)$ represents a time-dependent function to be determined, and $\phi(x)$ is the normalized linear mode shape function.

The single-mode Galerkin method only gives the nonlinear natural frequencies, but the multi-mode Galerkin method results in not only the nonlinear natural frequencies but also conditions of occurring the internal resonances. Since one of the main aims of the present research is to consider the state of internal resonances in nonlinear torsional vibration, the multi-mode Galerkin method is used.

Putting Eq. (25) into Eq. (12) results in the following equation

$$\left(\alpha_1\sum_{k=1}^{N}\sum_{j=1}^{N}\sum_{i=1}^{N}\frac{d\phi_i}{dx}\frac{d\phi_j}{dx}\frac{d^2\phi_k}{dx^2}\right)q_iq_jq_k + \left(\alpha_2\sum_{k=1}^{N}\sum_{j=1}^{N}\sum_{i=1}^{N}\phi_i\,\phi_j\,\phi_k\right)q_iq_jq_k + \left(\alpha_3\sum_{i=1}^{N}\frac{d^2\phi_i}{dx^2}\right) + \left(\alpha_4\sum_{k=1}^{N}\sum_{j=1}^{N}\sum_{i=1}^{N}\phi_i\frac{d\phi_j}{dx}\frac{d\phi_k}{dx}\right)q_iq_jq_k + \left(\alpha_4\sum_{k=1}^{N}\sum_{j=1}^{N}\sum_{i=1}^{N}\phi_i\,\phi_j\frac{d^2\phi_k}{dx^2}\right)q_iq_jq_k - \left(\alpha_5\sum_{i=1}^{N}\phi_i\right)\ddot{q}_\iota = 0 \quad (26)$$

Using the following dimensionless parameters,

$$X=\frac{x}{L};\quad \bar{q}=\frac{q}{q_{max}};\quad \bar{\phi}=\frac{\phi}{L}; \quad (27)$$

and multiplying Eq. (26) by the normalized linear mode shapes (Eqs. (20) and (22)) and integrating from X=0 to X=1, results in the following equation

$$\ddot{\bar{q}}_m+\omega_m^2\bar{q}_m - \varepsilon\sum_{i=1}\sum_{j=1}\sum_{k=1}\left(\left\{\frac{\alpha_1}{\alpha_5L^4}(\beta_1)_{mijk} + \frac{\alpha_2}{\alpha_5}(\beta_2)_{mijk} + \frac{\alpha_4}{\alpha_5L^2}\left((\beta_3)_{mijk} + (\beta_4)_{mijk}\right)\right\}\left(\bar{q}_i\bar{q}_j\bar{q_k}\right)\right){q_{max}}^2 = 0 \quad (28)$$

where q_{max} is the maximum amplitude of the time dependent function $q(t)$ and the parameters β_1, β_2, β_3 and β_4 are specified as:

$$\begin{aligned}(\beta_1)_{mijk}&=\int_0^1\left(\bar{\phi}_m\frac{d\bar{\phi}_i}{dX}\frac{d^2\bar{\phi}_k}{dX^2}\right)dX,\\ (\beta_2)_{mijk}&=\int_0^1\left(\bar{\phi}_m\bar{\phi}_i\bar{\phi}_j\bar{\phi}_k\right)dX,\\ (\beta_3)_{mijk}&=\int_0^1\left(\bar{\phi}_m\bar{\phi}_i\frac{d\bar{\phi}_j}{dX}\frac{d\bar{\phi}_k}{dX}\right)dX,\\ (\beta_4)_{mijk}&=\int_0^1\left(\bar{\phi}_m\bar{\phi}_i\bar{\phi}_j\frac{d^2\bar{\phi}_k}{dX^2}\right)dX.\end{aligned} \quad (29)$$

and

$$\begin{cases}\int_0^1\bar{\phi}_m(x)\bar{\phi}_i(x)dX=\delta_{im}\\ \int_0^1\bar{\phi}_m(x)\frac{d^2\bar{\phi}_i(x)}{dX^2}dX=-\lambda_m^2\delta_{im}\\ \omega_m^2=\frac{\alpha_3{\lambda_m}^2}{\alpha_5L^2}\end{cases} \quad (30)$$

In Eq. (30) $\lambda_m$and $\bar{\phi}(x)$ are defined as

$$\lambda_m=m\pi;\qquad \overline{\phi_m}=\sqrt{2}Sin(\lambda_mX) \quad (31)$$

$$\lambda_m=(2m-1)\frac{\pi}{2};\quad \overline{\phi_m}=\sqrt{2}Sin(\lambda_mX) \quad (32)$$

where Eqs. (31) and (32) are for fixed-fixed and fixed-free end conditions, respectively.

3. Solution Procedure

To solve the nonlinear equation, Eq. (28), the multiple-scale method is used. For this purpose, the small dimensionless parameter ε is introduced. Therefore, Eq. (28) can be written as follow

$$\bar{q}_m(t_i;\varepsilon)=\bar{q}_{m_0}(t_0,t_1)+\varepsilon\bar{q}_{m_1}(t_0,t_1)+\varepsilon^2\bar{q}_{m_2}(t_0,t_1)+\cdots \quad (33)$$

where $t_0 = t$ is the time scale that indicates oscillatory effect and

$$t_n=\varepsilon^n t \quad (34)$$

Substituting Eq. (33) into Eq. (28) and equating the coefficients with the same power results in the following differential equations:

$$\varepsilon^0:\quad {D_0}^2\bar{q}_{m_0}+{\omega_m}^2\bar{q}_{m_0}=0; \quad (35)$$

$$\varepsilon^1:\quad {D_0}^2\bar{q}_{m_1}+{\omega_m}^2\bar{q}_{m_1}=-2D_0D_1\bar{q}_{m_0}+\left(\frac{\alpha_1(\beta_1)_{mmmm}}{\alpha_5L^4}+\frac{\alpha_2(\beta_2)_{mmmm}}{\alpha_5}+\frac{\alpha_4}{\alpha_5L^2}\left((\beta_3)_{mmmm}+(\beta_4)_{mmmm}\right)\right){\bar{q}_{m_0}}^3{q_{max}}^2; \quad (36)$$

$$\varepsilon^2:\quad {D_0}^2\bar{q}_{m_2}+{\omega_m}^2\bar{q}_{m_2}=-\left({D_1}^2+2D_0D_2\right)\bar{q}_{m_0}-2D_0D_1\bar{q}_{m_1}+{\bar{q}_{m_0}}^2{q_{max}}^2\sum_{p=1}^{3}\bar{q}_{(p,1)}\left\{\frac{\alpha_1}{L^4\alpha_5}\left((\beta_1)_{mmmp}+(\beta_1)_{mmpm}+(\beta_1)_{mpmm}\right)+\frac{\alpha_2}{\alpha_5}\left((\beta_2)_{mmmp}+(\beta_2)_{mmpm}+(\beta_2)_{mpmm}\right)+\frac{\alpha_4}{\alpha_5L^2}\left((\beta_3)_{mmmp}+(\beta_3)_{mmpm}+(\beta_3)_{mpmm}+(\beta_4)_{mmmp}+(\beta_4)_{mmpm}+(\beta_4)_{mpmm}\right)\right\}; \quad (37)$$

where $D_i = \frac{\partial}{\partial \bar{t}_i}$. A general solution for Eq. (35) can be written as

$$\bar{q}_{m_0} = A_m e^{i\omega_m t_0} + \bar{A}_m\, e^{-i\omega_m t_0} \tag{38}$$

$$\bar{q}_{n_0} = 0 \quad for \quad n \neq m \tag{39}$$

A_m is a complex function and will be determined later, and $\bar{A}_m$ is the complex conjugate of A_m.

Substituting $\bar{q}_{m_0}$ and $\bar{q}_{n_0}$ into Eqs. (36) results in

$$\begin{aligned}
&{D_0}^2\bar{q}_{m_1} + {\omega_m}^2\bar{q}_{m_1} \\
&= -(D_1A_m)\left(2i\omega_m e^{i\omega_m t_0}\right) \\
&+ {q_{max}}^2\left(\left(\frac{\alpha_1(\beta_1)_{mmmm}}{\alpha_5 L^4} + \frac{\alpha_2(\beta_2)_{mmmm}}{\alpha_5}\right.\right. \\
&+ \frac{\alpha_4}{\alpha_5 L^2}\left((\beta_3)_{mmmm}\right. \\
&\left.\left.\left. + (\beta_4)_{mmmm}\right)\right){A_m}^3 e^{3i\omega_m t_0}\right. \\
&+ 3\left(\frac{\alpha_1(\beta_1)_{mmmm}}{\alpha_5 L^4} + \frac{\alpha_2(\beta_2)_{mmmm}}{\alpha_5}\right. \\
&+ \frac{\alpha_4}{\alpha_5 L^2}\left((\beta_3)_{mmmm}\right. \\
&\left.\left.\left. + (\beta_4)_{mmmm}\right)\right){A_m}^2\bar{A}_m e^{i\omega_m t_0}\right) + CC \\
&{D_0}^2\bar{q}_{n_1} + {\omega_m}^2\bar{q}_{n_1} \\
&= {q_{max}}^2\left(\left(\frac{\alpha_1(\beta_1)_{mmmm}}{\alpha_5 L^4} + \frac{\alpha_2(\beta_2)_{mmmm}}{\alpha_5}\right.\right. \\
&+ \frac{\alpha_4}{\alpha_5 L^2}\left((\beta_3)_{mmmm}\right. \\
&\left.\left.\left. + (\beta_4)_{mmmm}\right)\right){A_m}^3 e^{3i\omega_m t_0}\right. \\
&+ 3\left(\frac{\alpha_1(\beta_1)_{mmmm}}{\alpha_5 L^4} + \frac{\alpha_2(\beta_2)_{mmmm}}{\alpha_5}\right. \\
&+ \frac{\alpha_4}{\alpha_5 L^2}\left((\beta_3)_{mmmm}\right. \\
&\left.\left.\left. + (\beta_4)_{mmmm}\right)\right){A_m}^2\bar{A}_m e^{i\omega_m t_0}\right) + CC
\end{aligned} \tag{40, 41}$$

where CC is the complex conjugate of the preceding terms. Since the general solution of Eq. (40) is similar to Eq. (35), the following term causes a resonant effect and hence called the secular term

$$\left(-(D_1A_m)(2i\omega_m) + 3\left(\frac{\alpha_1(\beta_1)_{mmmm}}{\alpha_5 L^4} + \frac{\alpha_2(\beta_2)_{mmmm}}{\alpha_5} + \frac{\alpha_4}{\alpha_5 L^2}\left((\beta_3)_{mmmm} + (\beta_4)_{mmmm}\right)\right){A_m}^2\bar{A}_m\right)e^{i\omega_m t_0}$$

To prevent the resonant, we should have

$$\left(-(D_1A_m)(2i\omega_m) + 3\left(\frac{\alpha_1(\beta_1)_{mmmm}}{\alpha_5 L^4} + \frac{\alpha_2(\beta_2)_{mmmm}}{\alpha_5} + \frac{\alpha_4}{\alpha_5 L^2}\left((\beta_3)_{mmmm} + (\beta_4)_{mmmm}\right)\right){A_m}^2\bar{A}_m\right) = 0 \tag{42}$$

Then, the solution of Eqs. (40) and (41) becomes

$$\begin{aligned}
&\bar{q}_{m_1} \\
&= -\left(\frac{\alpha_1(\beta_1)_{mmmm}}{\alpha_5 L^4} + \frac{\alpha_2(\beta_2)_{mmmm}}{\alpha_5}\right. \\
&+ \frac{\alpha_4}{\alpha_5 L^2}\left((\beta_3)_{mmmm}\right. \\
&\left.\left. + (\beta_4)_{mmmm}\right)\right)\frac{{q_{max}}^2}{8{\omega_m}^2}{A_m}^3 e^{3i\omega_m t_0}
\end{aligned} \tag{43}$$

$$\begin{aligned}
&\bar{q}_{n_1} \\
&= \left(\frac{\alpha_1(\beta_1)_{mmmm}}{\alpha_5 L^4} + \frac{\alpha_2(\beta_2)_{mmmm}}{\alpha_5}\right. \\
&\left. + \frac{\alpha_4}{\alpha_5 L^2}\left((\beta_3)_{mmmm} + (\beta_4)_{mmmm}\right)\right) \\
&\times \frac{{q_{max}}^2}{\left({\omega_n}^2 - 9{\omega_m}^2\right)}{A_m}^3 e^{3i\omega_m t_0} \\
&+ 3\left(\frac{\alpha_1(\beta_1)_{mmmm}}{\alpha_5 L^4} + \frac{\alpha_2(\beta_2)_{mmmm}}{\alpha_5}\right. \\
&\left. + \frac{\alpha_4}{\alpha_5 L^2}\left((\beta_3)_{mmmm} + (\beta_4)_{mmmm}\right)\right) \\
&\times \frac{{q_{max}}^2}{\left({\omega_n}^2 - {\omega_m}^2\right)}{A_m}^2\bar{A}_m e^{i\omega_m t_0}
\end{aligned} \tag{44}$$

Now, A_m is expressed in the polar form

$$A_m = \frac{1}{2}a_m e^{ib_m} \tag{45}$$

in which a and b indicate real variables. Putting Eq. (45) into Eq. (42) and separating the imaginary and real parts equal to zero, results in the following equations

- Real part

$$\begin{aligned}
&\omega_m b'_m a_m \\
&+ {q_{max}}^2\left(\frac{3}{8}{a_m}^3\right)\left(\frac{\alpha_1(\beta_1)_{mmmm}}{\alpha_5 L^4}\right. \\
&+ \frac{\alpha_2(\beta_2)_{mmmm}}{\alpha_5} \\
&\left. + \frac{\alpha_4}{\alpha_5 L^2}\left((\beta_3)_{mmmm} + (\beta_4)_{mmmm}\right)\right) = 0
\end{aligned} \tag{46}$$

- Imaginary part $\quad -i\omega_m a'_m = 0$

From Eq. (46), it is possible to obtain

$$b_m = -\frac{{q_{max}}^2}{\omega_m}\left(\frac{3}{8}{a_m}^2\right)\left(\frac{\alpha_1(\beta_1)_{mmmm}}{\alpha_5 L^4} + \frac{\alpha_2(\beta_2)_{mmmm}}{\alpha_5} + \frac{\alpha_4}{\alpha_5 L^2}((\beta_3)_{mmmm} + (\beta_4)_{mmmm})\right)t_1 + b_{m_0} \quad (47)$$

$a_m = Constant.$

Substituting Eq. (47) into Eq. (45) yields the following equation

$$A_m = \frac{a_m}{2} e^{i\left(\begin{array}{c} b_{m_0} - \frac{{q_{max}}^2}{\omega_m}\left(\frac{3}{8}{a_m}^2\right)\times \\ \left(\frac{\alpha_1(\beta_1)_{mmmm}}{\alpha_5 L^4} + \frac{\alpha_2(\beta_2)_{mmmm}}{\alpha_5} + \right. \\ \left. \frac{\alpha_4}{\alpha_5 L^2}((\beta_3)_{mmmm} + (\beta_4)_{mmmm})\right)t_1 \end{array}\right)} \quad (48)$$

Also, $\bar{q}_m$ and $\bar{q}_n$ are obtained as

$$\begin{aligned} \bar{q}_m &= A_m e^{i\omega_m t_0} \\ &- \varepsilon\left(\frac{\alpha_1(\beta_1)_{mmmm}}{\alpha_5 L^4} + \frac{\alpha_2(\beta_2)_{mmmm}}{\alpha_5} + \frac{\alpha_4}{\alpha_5 L^2}((\beta_3)_{mmmm} + (\beta_4)_{mmmm})\right)\frac{{q_{max}}^2}{8{\omega_m}^2}{A_m}^3 e^{3i\omega_m t_0} + CC \end{aligned} \quad (49)$$

$$\begin{aligned} \bar{q}_n &= \varepsilon\left(\left(\frac{\alpha_1(\beta_1)_{mmmm}}{\alpha_5 L^4} + \frac{\alpha_2(\beta_2)_{mmmm}}{\alpha_5} + \frac{\alpha_4}{\alpha_5 L^2}((\beta_3)_{mmmm} + (\beta_4)_{mmmm})\right) \times \frac{{q_{max}}^2}{\left({\omega_n}^2 - 9{\omega_m}^2\right)}{A_m}^3 e^{3i\omega_m t_0}\right) + \\ &\varepsilon\left(3\left(\frac{\alpha_1(\beta_1)_{mmmm}}{\alpha_5 L^4} + \frac{\alpha_2(\beta_2)_{mmmm}}{\alpha_5} + \frac{\alpha_4}{\alpha_5 L^2}((\beta_3)_{mmmm} + (\beta_4)_{mmmm})\right) \times \frac{{q_{max}}^2}{({\omega_n}^2 - {\omega_m}^2)}{A_m}^2 \bar{A}_m e^{i\omega_m t_0}\right) \end{aligned} \quad (50)$$

By considering Eq. (48), Eqs. (49) and (50) can be rewritten as:

$$\begin{aligned} \bar{q}_m &= a_m \cos\theta \\ &- \varepsilon\left(\left(\frac{\alpha_1(\beta_1)_{mmmm}}{\alpha_5 L^4} + \frac{\alpha_2(\beta_2)_{mmmm}}{\alpha_5} + \frac{\alpha_4}{\alpha_5 L^2}((\beta_3)_{mmmm} + (\beta_4)_{mmmm})\right)\frac{{a_m}^3}{32{\omega_m}^2}{q_{max}}^2\right)\cos(3\theta) \\ &+ \cdots \end{aligned} \quad (51)$$

$$\begin{aligned} \bar{q}_n &= \varepsilon\left(3\left(\frac{\alpha_1(\beta_1)_{mmmm}}{\alpha_5 L^4} + \frac{\alpha_2(\beta_2)_{mmmm}}{\alpha_5} + \frac{\alpha_4}{\alpha_5 L^2}((\beta_3)_{mmmm} + (\beta_4)_{mmmm})\right) \times \frac{{a_m}^3}{4({\omega_n}^2 - {\omega_m}^2)}{q_{max}}^2\cos(\theta)\right. \\ &\left. + \left(\frac{\alpha_1(\beta_1)_{mmmm}}{\alpha_5 L^4} + \frac{\alpha_2(\beta_2)_{mmmm}}{\alpha_5} + \frac{\alpha_4}{\alpha_5 L^2}((\beta_3)_{mmmm} + (\beta_4)_{mmmm})\right) \times \frac{{a_m}^3}{4\left({\omega_n}^2 - 9{\omega_m}^2\right)}{q_{max}}^2\cos(3\theta)\right) \end{aligned} \quad (52)$$

where

$$\begin{aligned} &\theta = \omega_{Nm} t + b_{m_0}; \\ &\omega_{Nm} = \omega_m - \\ &\frac{{q_{max}}^2}{\omega_m}\left(\frac{3}{8}{a_m}^2\right)\left(\frac{\alpha_1(\beta_1)_{mmmm}}{\alpha_5 L^4} + \right. \\ &\left. \frac{\alpha_2(\beta_2)_{mmmm}}{\alpha_5} + \frac{\alpha_4}{\alpha_5 L^2}((\beta_3)_{mmmm} + \right. \\ &\left. (\beta_4)_{mmmm})\right)\varepsilon + b_{m_0}; \end{aligned} \quad (53)$$

and ω_{Nm} and ω_m are nonlinear and linear natural frequencies, respectively. To satisfy the initial conditions ($\bar{q}_m(0) = 1$; $\dot{\bar{q}}_m(0) = 0$) in Eq. (47), the error associated with the second order expansion should be considered. In Addition, because ε is a bookkeeping device, we set it equal to unity. These result in $b_{m_0} = 0$; $a_m = 1$. Eq. (52) shows that there are two cases in which the internal resonances occur, one-to-one ($\omega_n = \omega_m$) and three-to-one ($\omega_n = 3\omega_m$).

4. Numerical Results

In the following, the influence of surface effects, the amplitude of nonlinear vibrations, the frequency number, the radius, and the length of the nanorod on the linear and nonlinear frequencies of the nanorod are investigated. The bulk and the surface elastic properties of aluminum and silicon are listed in Table 1. It should be mentioned that the crystallographic

direction of aluminum is [1 1 1], and the crystallographic direction of silicon is [1 0 0].

To display the high accuracy of the present results, a direct comparison has been conducted with the results obtained by Jamali Shakhlavi et al. [39] and Setoodeh et al. [40] in Table 2. From this table, it can be found that the results presented in this study are closely matched with those given by [39,40]. The slight difference between the results of the present study with those of reference [40] is the method of solution. Setoodeh et al. [40] used the Homotopy Analysis method while the present study used the method of multiple scale.

To show better the effects of surface components on the natural torsional frequencies of nanorods, the frequency ratio in the form of Eq. (54) is used. This equation states that if the frequency ratio is more than one, the surface components have an accumulative effect and vice versa. Also, for the frequency ratio equal to one, surface components do not affect the natural torsional frequencies of nanorods. The frequency ratio is defined as

$$FR = \frac{f_s}{f_c} \tag{54}$$

where f_s and f_c are the natural torsional frequency of nanorod with surface energy effects, and the natural torsional frequency of nanorod, respectively.

The influence of surface parameters on the torsional vibration of nanorod is listed in Table 3 for various radii and amplitudes of vibration. According to this table, the following results can be deduced. First, it is seen that in the case of linear torsional vibration (q_{max}=0), both the surface density and the surface Lamé constants decrease the natural torsional frequencies for different frequency numbers, various values of nanorod radii, and two boundary conditions i.e., fixed-fixed and fixed-free. This result is valid in the nonlinear case only for the surface density effect. While it is observed that the surface Lamé constants have different effects on nonlinear torsional frequencies. In other words, the effect of surface Lamé constants on the nonlinear torsional frequencies depends on the vibration amplitude, the material of the nanorod, mode number, and radius of the nanorod. It is worth mentioning that the reason for decreasing effect of the surface density is increasing the kinetic energy of the nanorod due to considering the surface density. As known, the frequency and the kinetic energy are inversely related.

Then, Table 3 shows that the effect of surface density on torsional frequencies is different only for various values of nanorod radius. This means that the surface density decreases the torsional frequencies with the same percent for various boundary conditions, mode numbers, and amplitudes of vibration. But, this is not the case for the surface density effect on torsional frequencies for multiple values of nanorod radius. This implies that by increasing the nanorod radius, the surface density effect decreases. This is due to the fact that by increasing the nanorod radius, the energy stored in the bulk grows faster than the one on the surface. It is also observed from Table 3 that the decreasing effect of the surface density on the torsional frequencies of nanorod made of aluminum is more in comparison with the one made of silicon. The reason for this is that the value of the surface density of aluminum is greater than the one of silicon.

Table 1. Bulk and the surface elastic properties of Aluminum and Silicon

Material	Bulk elastic properties		Surface elastic properties		
	$G(GPa)$	$\rho\left({}^{kg}/_{m^3}\right)$	$\bar{\rho}\left({}^{kg}/_{m^3}\right)$	$\bar{\lambda}({}^{N}/_{m})$	$\bar{\mu}({}^{N}/_{m})$
Al	28.5	2700	$10^{-7}\times5.46$	6.842	-0.367
Si	86	2370	$10^{-7}\times3.17$	-4.494	-2.7779

Table 2. Comparison of nonlinear torsional frequencies (GHz) for various lengths and mode numbers, μ, and all surface parameters considered zero.

Amplitude of vibration (D/π)	Length (nm)	Mode number	Setoodeh et al. [40]	Jamali et al. [39]	Present study
0.001	10	1st	167.422	167.409	167.409
		2nd	363.744	363.430	363.430
	15	1st	109.738	109.736	109.736
		2nd	228.380	228.331	228.331
0.010	10	1st	441.133	434.047	434.047
		2nd	1672.54	1639.00	1639.00
	15	1st	212.00	209.533	209.533
		2nd	760.65	746.79	746.79

Next, it is focused on the effect of surface Lamé constants on the torsional frequencies. First, it is observed that impact of the surface Lamé constants is different in linear and nonlinear cases. In linear vibration, decreasing effect of surface Lamé constants is the same for both types of boundary conditions, i.e., fixed-fixed and fixed-free, while this is not the case in nonlinear vibration. For a given radius value, the decreasing effect of the surface Lamé constants is also the same at all frequency numbers in the linear vibration. In the nonlinear vibration case, the decreasing effect of the surface Lamé constants differs with changing the type of boundary condition, the value of the vibration amplitude, the value of nanorod thickness, and the frequency number. By increasing the value of the amplitude of vibration, the frequency ratio value becomes more remarkable. This means that the nonlinearity has an increasing effect on the torsional frequencies, and this effect becomes more by increasing the vibration amplitude. This result is also observed for various values of the nanorod radius and frequency number. The final point regarding the surface Lamé constants effect is that by increasing the nanorod radius, two phenomena occur. Firstly, the decreasing effect of surface Lamé constants decreases, which is due to the fact that by increasing the nanorod radius, the energy stored in the bulk grows faster than the one on the surface. Secondly, the increasing effect of nonlinearity decreases due to the thickening of the nanorod.

Finally, it is focused on the simultaneous effect of surface density and the surface Lamé constants. It is observed from Table 3 that when effects of both the surface density and the surface Lamé constants are considered, the values of all frequency ratios become more minor than those when one of them is considered. This implies that the decreasing effect of surface parameters becomes more when they are considered simultaneously compared to the case they are solely considered.

Tables 4 and 5 study the influences of the surface effect on the internal resonances of the nanorods. It is crucial to learn these values to prevent undetected resonances in nanostructures. The length of the nanorods is chosen larger than 5nm and less than 40nm to keep a sensible shape for the nanorods. It is seen from these tables that the ratios of internal resonances for classical nanorods are independent of n, m, and q_{max} and for both materials and boundary conditions. Besides, it is observed that considering the surface effect results in lower internal resonance ratios for all values, and they are independent of the vibration amplitude, but they are related to the type of ends conditions and mode number.

Table 3. Nonlinear torsional frequency ratios for various cases

R (nm)	n	q_{max}	B.C. type	only surface density		only surface Lamé		both surface density and Lamé	
				Al	Si	Al	Si	Al	Si
1	1	0	Fi-Fi	0.7435	0.8071	0.9457	0.4680	0.7031	0.3777
			Fi-Fr	0.7435	0.8071	0.9457	0.4680	0.7031	0.3777
		0.05	Fi-Fi	0.7435	0.8071	0.9744	0.8966	0.7245	0.7237
			Fi-Fr	0.7435	0.8071	1.0064	1.3746	0.7483	1.1095
		0.1	Fi-Fi	0.7435	0.8071	1.0064	1.3745	0.7483	1.1094
			Fi-Fr	0.7435	0.8071	1.0299	1.7253	0.7657	1.3925
	5	0	Fi-Fi	0.7435	0.8071	0.9457	0.4680	0.7031	0.3777
			Fi-Fr	0.7435	0.8071	0.9457	0.4680	0.7031	0.3777
		0.05	Fi-Fi	0.7435	0.8071	0.9473	0.4929	0.7044	0.3979
			Fi-Fr	0.7435	0.8071	0.9477	0.4983	0.7046	0.4022
		0.1	Fi-Fi	0.7435	0.8071	0.9520	0.5627	0.7078	0.4541
			Fi-Fr	0.7435	0.8071	0.9533	0.5819	0.7088	0.4697
2	1	0	Fi-Fi	0.8438	0.8882	0.9732	0.7807	0.8212	0.6934
			Fi-Fr	0.8438	0.8882	0.9732	0.7807	0.8212	0.6934
		0.05	Fi-Fi	0.8438	0.8882	0.9777	0.8221	0.8250	0.7302
			Fi-Fr	0.8438	0.8882	0.9872	0.9092	0.8330	0.8076
		0.1	Fi-Fi	0.8438	0.8882	0.9872	0.9093	0.8330	0.8077
			Fi-Fr	0.8438	0.8882	1.0027	1.0524	0.8461	0.9348
	5	0	Fi-Fi	0.8438	0.8882	0.9732	0.7807	0.8212	0.6934
			Fi-Fr	0.8438	0.8882	0.9732	0.7807	0.8212	0.6934
		0.05	Fi-Fi	0.8438	0.8882	0.9735	0.7834	0.8215	0.6958
			Fi-Fr	0.8438	0.8882	0.9735	0.7837	0.8215	0.6961
		0.1	Fi-Fi	0.8438	0.8882	0.9744	0.7912	0.8222	0.7028
			Fi-Fr	0.8438	0.8882	0.9745	0.7923	0.8223	0.7037

Table 4. Internal resonances ratios for Al nanorod and various cases (R = 1.5nm)

Fixed-Fixed						Fixed-Free					
n	m	q_{max}	Length (nm)	Ratio		n	m	q_{max}	Length (nm)	Ratio	
				Classic	With surface effect					Classic	With surface effect
1	4	0.06	23.27	3	2.953	1	3	0.06	16.28	3	2.926
1	4	0.07	19.98	3	2.953	1	3	0.07	13.97	3	2.926
1	4	0.08	17.54	3	2.953	1	3	0.08	12.25	3	2.926
1	4	0.09	15.66	3	2.953	1	3	0.09	10.91	3	2.926
1	4	0.1	14.18	3	2.953	1	3	0.1	9.85	3	2.926
1	5	0.06	32.57	3	2.923	1	4	0.06	22.79	3	2.895
1	5	0.07	27.95	3	2.923	1	4	0.07	19.55	3	2.895
1	5	0.08	24.50	3	2.923	1	4	0.08	17.13	3	2.895
1	5	0.09	21.83	3	2.923	1	4	0.09	15.25	3	2.895
1	5	0.1	19.71	3	2.923	1	4	0.1	13.76	3	2.895
1	6	0.06	39.64	3	2.908	1	5	0.06	27.76	3	2.878
1	6	0.07	34.01	3	2.908	1	5	0.07	23.81	3	2.878
1	6	0.08	29.80	3	2.908	1	5	0.08	20.86	3	2.878
1	6	0.09	26.54	3	2.908	1	5	0.09	18.57	3	2.878
1	6	0.1	23.95	3	2.908	1	5	0.1	16.76	3	2.878

Table 5. Frequency ratios of Si nanorod for different cases (R = 1.5nm)

Fixed-Fixed						Fixed-Free					
n	m	q_{max}	Length (nm)	Ratio		n	m	q_{max}	Length (nm)	Ratio	
				Classic	With surface effect					Classic	With surface effect
1	4	0.06	23.27	3	2.873	1	3	0.06	16.28	3	2.803
1	4	0.07	19.98	3	2.873	1	3	0.07	13.97	3	2.803
1	4	0.08	17.54	3	2.873	1	3	0.08	12.25	3	2.803
1	4	0.09	15.66	3	2.873	1	3	0.09	10.91	3	2.803
1	4	0.1	14.18	3	2.873	1	3	0.1	9.85	3	2.803
1	5	0.06	32.57	3	2.803	1	4	0.06	22.79	3	2.727
1	5	0.07	27.95	3	2.803	1	4	0.07	19.55	3	2.727
1	5	0.08	24.50	3	2.803	1	4	0.08	17.13	3	2.727
1	5	0.09	21.83	3	2.803	1	4	0.09	15.25	3	2.727
1	5	0.1	19.17	3	2.803	1	4	0.1	13.76	3	2.727
1	6	0.06	39.64	3	2.758	1	5	0.06	27.76	3	2.685
1	6	0.07	34.01	3	2.758	1	5	0.07	23.81	3	2.685
1	6	0.08	29.80	3	2.758	1	5	0.08	20.86	3	2.685
1	6	0.09	26.54	3	2.758	1	5	0.09	18.57	3	2.685
1	6	0.1	23.95	3	2.758	1	5	0.1	16.76	3	2.685

It is also observed from Tables 4 and 5 that for higher frequency numbers, the internal resonance conditions are observed for large nanorod lengths, and at higher amplitude of vibrations, the more internal resonance conditions occur for smaller nanorod lengths. Moreover, by considering the surface effects, for a higher frequency number, changes in the internal resonance conditions become greater. This result is true for both boundary conditions (i.e., fi-fi and fi-fr) and both materials (i.e., Al and Si). Without considering the surface energy effect, the internal resonances for the fi-fr end condition occur at frequencies with closer mode numbers and shorter nanorod lengths, compared to the fi-fi boundary condition. Changes in the internal resonance conditions of the nanorod with the fi-fr boundary condition are more than the fi-fi

boundary condition when the surface effects are considered. Without considering the surface energy effects and under the same conditions, the internal resonance conditions are the same for both materials. However, when surface effects are considered, changes in internal resonance conditions for Si nanorods are more significant than Al nanorods. This is due to the difference between the values of the surface effect components of Al and Si. This difference highlights the importance of investigating surface effects on the internal resonances.

Figure 2 displays the change of the nonlinear natural frequency versus the nanorod length for two different boundary conditions, i.e., fi-fi and fi-fr, and for various surface effect parameters, at $q_{max} = 0.01$ and $R = 1\ nm$. It is evident for both boundary conditions, increasing in length of nanorod leads to a dramatic decrease in all nonlinear natural frequencies, which shows the decrease in length effects. The decrease in the distance among the curves is due to the reduction in the ratio of energy stored at the surface to the energy stored in the volume. Also, it is seen that by considering $\bar{\mu}$ and $\bar{\rho}$, all natural frequencies are lessened. This may be due to considering $\bar{\mu}$ in which the stiffness of nanorod falls off and taking into account $\bar{\rho}$ results in an increase in the nanorod mass. Other results that can be seen from these figures confirm the results previously stated in Tables 3-5 and are avoided to prevent duplication.

In the present paragraph, the effect of radius on the first natural frequency of the aluminum and silicon nanorods for two values of q_{max} and different surface parameters are presented in Figs. 3a-3d. It is observed that with increasing radius, the natural frequency for both boundary conditions and both materials increases gradually except for the classical nanorod with $q_{max} = 0$. This implies the independency of nanorods' classical natural frequency from their radius. When the surface energy effect is considered, the linear and nonlinear frequencies of nanorods are related to the nanorod radius. For both boundary conditions and both materials properties, linear frequencies of nanorod without considering the surface energy effect are independent of the nanorod radius, whereas nonlinear frequencies of nanorod without considering the surface energy effect are dependent on the radius of the nanorod. It should be noted that since the Lamé constants of Si are positive, unlike other surface constants that have a decreasing effect on frequency, this parameter has a positive effect. The behavior of the nonlinear frequency curve in terms of the radius can be different from other constants by considering the effect of this constant. The difference in the behavior of the curve certainly depends on the amplitude of the nonlinear vibrations of the nanorod.

The variation of the first natural frequency of the aluminum and silicon nanorods against the nanorod amplitude for various surface parameters is presented in Figs. 4a and 4b. It is seen that by increasing the vibration amplitude the system's nonlinearity increases and leads to the rise of the natural frequency for both Al and Si nanorods. Also, it is obvious increasing frequency because the rise in the vibration amplitude is greater for nanorods with fixed-free boundary condition than that of nanorods with fixed-fixed boundary condition.

In all figures, it is seen that the natural frequencies obtained for the fixed-fixed end condition are higher than those predicted for the fixed-free boundary conditions. Actually, the stiffness of fixed-fixed nanorods is more than the fixed-free nanorods, and thus the frequencies are increased.

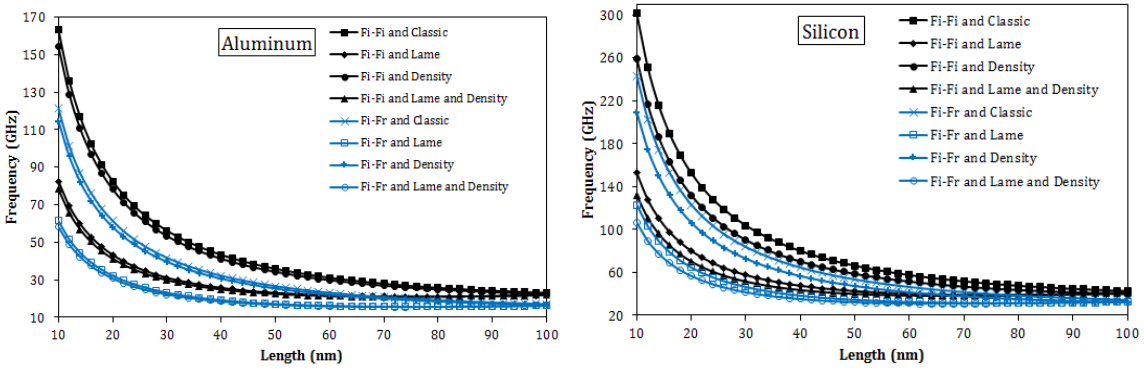

Fig. 2. Variations of the nonlinear natural frequency with the length of nanorod for two boundary conditions, fi–fi, and fi–fr at R = 0.5 nm.

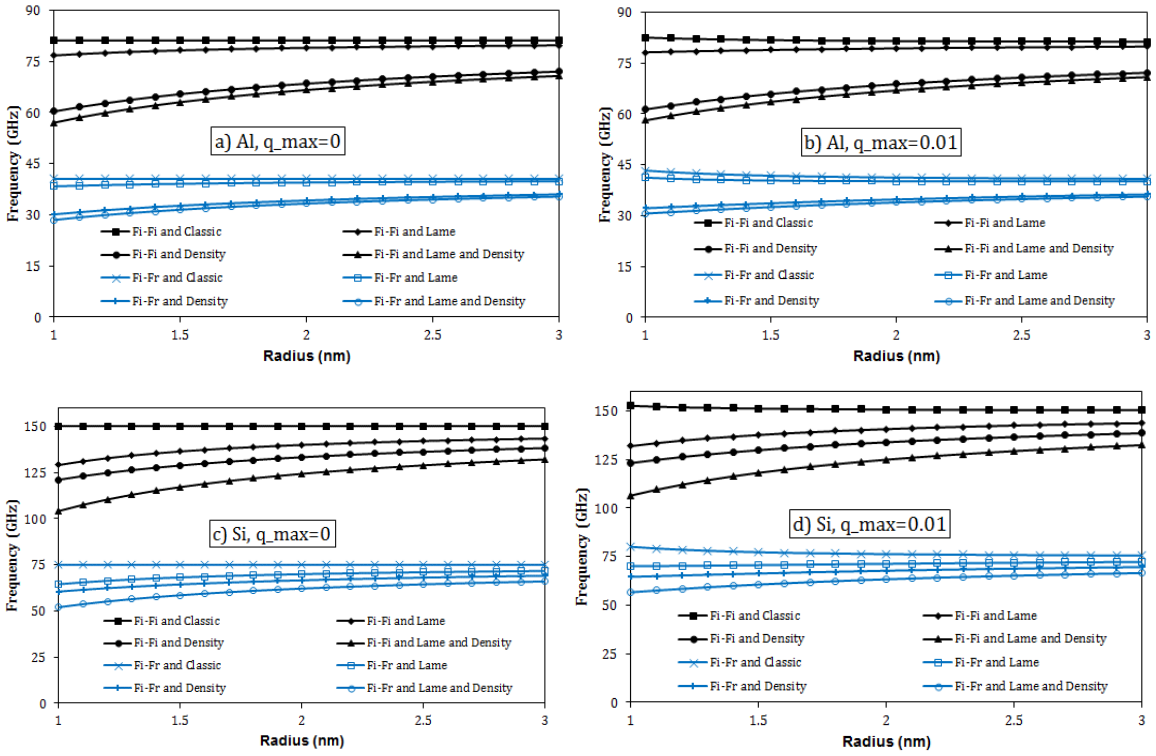

Fig. 3. Variations of the nonlinear natural frequency with the radius of aluminum nanorod for two boundary conditions, fi–fi, and fi–fr at L = 20 nm.

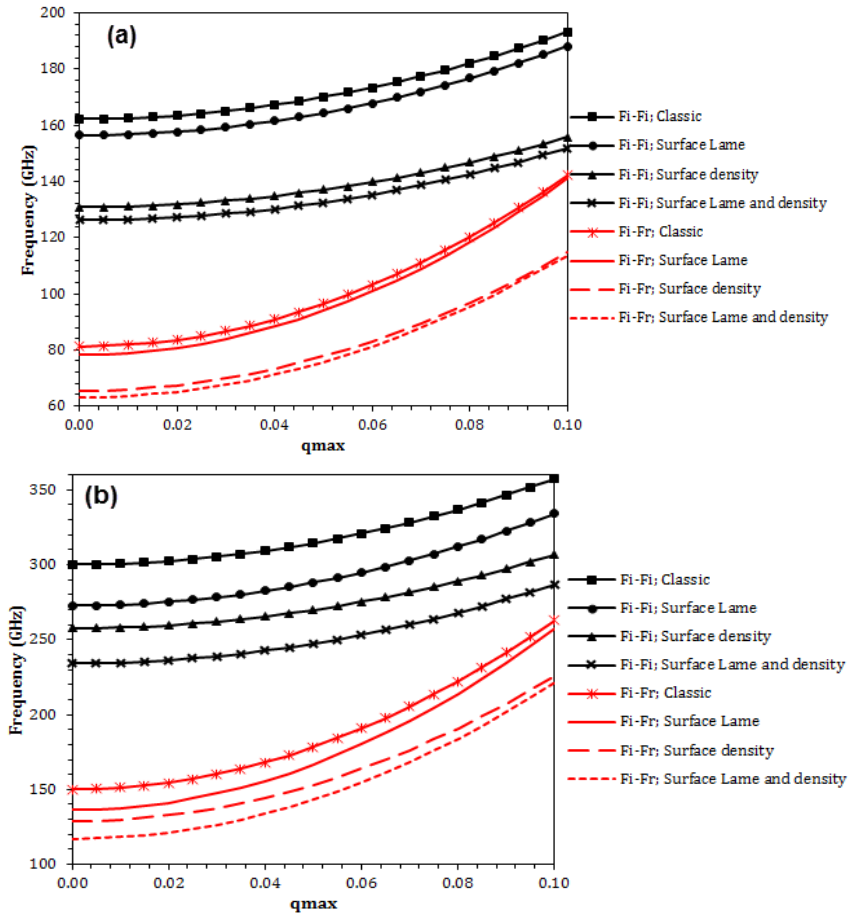

Fig. 4. Variations of first natural frequency for Al nanorod against amplitude R=1.5 nm; L=10 nm (a) Al, (b) Si.

5. Conclusions

In this paper, torsional vibrations of nanorods were investigated by considering the surface effects and the fixed-fixed and fixed-free end conditions. It is found that for various amplitudes of vibration, different frequency numbers, and both boundary conditions, the surface density has a decreasing effect on the torsional vibration of nanorod while considering only surface Lame, can have a decreasing or increasing effect on the torsional frequencies of nanorods. When both surface density and Lame constants are considered, a decreasing effect on the natural torsional frequency of nanorod is seen, and this reduction is greater than when the surface density or surface Lame is deemed to be alone. Also, when surface effects are considered, changes in internal resonance conditions for Si nanorods are more significant than Al nanorods.

Reference

[1] Hosseini–Hashemi, S., Fakher, M. and Nazemnezhad, R., 2013. Surface effects on free vibration analysis of nanobeams using nonlocal elasticity: a comparison between Euler-Bernoulli and Timoshenko. *Journal of Solid Mechanics*, *5*, pp.290-304.

[2] Hosseini-Hashemi, S., Nahas, I., Fakher, M. and Nazemnezhad, R., 2014. *Surface effects on free vibration of piezoelectric functionally graded nanobeams using nonlocal elasticity*. *Acta Mechanica*, 225, pp.1555-1564.

[3] Hosseini-Hashemi, S., Zare, M. and Nazemnezhad, R., 2013. An exact analytical approach for free vibration of Mindlin rectangular nano-plates via nonlocal elasticity. *Composite Structures, 100,* pp.290-299.

[4] Jandaghian, A. and Rahmani, O., 2016. An analytical solution for free vibration of piezoelectric nanobeams based on a nonlocal elasticity theory. *Journal of Mechanics*, *32*, pp.143-151.

[5] Jandaghian, A.A. and Rahmani, O, 2017. Buckling analysis of multi-layered graphene sheets based on a continuum mechanics model. *Applied Physics A*, *123*, pp.324.

[6] Jandaghian, A.A. and Rahmani, O., 2015. On the buckling behavior of piezoelectric nanobeams: An exact solution. *Journal of Mechanical Science and Technology*, *29*, pp.3175-3182.

[7] Gurtin, M.E. and Ian Murdoch, A., 1975. A continuum theory of elastic material surfaces. *Archive for Rational Mechanics and Analysis*, *57*, pp.291-323.

[8] Gurtin, M.E., Weissmüller, J. and Larché, F., 1998. A general theory of curved deformable interfaces in solids at equilibrium. *Philosophical Magazine A*, *78*, pp.1093-1109.

[9] Bar On, B., Altus, E. and Tadmor, E. B., 2010. Surface effects in non-uniform nanobeams: Continuum vs. atomistic modeling. *International Journal of Solids and Structures*, *47*, pp.1243-1252.

[10] Wang, G.-F. and Feng, X.-Q., 2007. Effects of surface elasticity and residual surface tension on the natural frequency of microbeams. *Applied Physics Letters*, *90*, pp.231904.

[11] Ansari, R. and Sahmani, S., 2011. Bending behavior and buckling of nanobeams including surface stress effects corresponding to different beam theories. *International Journal of Engineering Science*, *49*, pp.1244-1255.

[12] Ansari, R., Mohammadi, V., Faghih Shojaei, M., Gholami, R. and Sahmani, S., 2014. Postbuckling analysis of Timoshenko nanobeams including surface stress effect. *International Journal of Engineering Science*, *75*, pp.1-10.

[13] Abbasion, S., Rafsanjani, A., Avazmohammadi, R. and Farshidianfar, A., 2009. Free vibration of microscaled Timoshenko beams. *Applied Physics Letters*, *95*, pp.143122.

[14] Wang, L., 2010. Vibration analysis of fluid-conveying nanotubes with consideration of surface effects. *Physica E: Low-dimensional Systems and Nanostructures*, *43*, pp.437-439.

[15] Farshi, B., Assadi, A. and Alinia-Ziazi, A., 2010. Frequency analysis of nanotubes with consideration of surface effects. *Applied Physics Letters*, *96*, pp.093105.

[16] He, J. and Lilley C.M., 2008. Surface effect on the elastic behavior of static bending nanowires. *Nano letters*, 8, pp.1798-1802.

[17] Fang, X., Zhu, Ch., Liu, J. and Liu, X., 2018. Surface energy effect on free vibration of nano-sized piezoelectric double-shell Structures. *Physica B: Condensed Matter,* 529, pp.41-56.

[18] Nazemnezhad, R., Salimi, M., Hosseini Hashemi, S. and Asgharifard Sharabiani, P., 2012. An analytical study on the nonlinear free vibration of nanoscale beams incorporating surface density effects. *Composites Part B: Engineering*, *43*, pp.2893-2897.

[19] Ansari, R., Mohammadi, V., Shojaei, M. F., Gholami, R. and Rouhi, H., 2014. Nonlinear vibration analysis of Timoshenko nanobeams based on surface stress elasticity theory. *European Journal of Mechanics-A/Solids*, *45*, pp.143-152.

[20] Asgharifard Sharabiani, P. and Haeri Yazdi, M. R., 2013. Nonlinear free vibrations of

functionally graded nanobeams with surface effects. *Composites Part B: Engineering*, *45*, pp.581-586.

[21] Zhu, Ch., Fang, X. and Liu, J., 2020. A new approach for smart control of size-dependent nonlinear free vibration of viscoelastic orthotropic piezoelectric doubly-curved nanoshells. *Applied Mathematical Modelling,* 77, pp.137-168.

[22] Zhu, Ch., Fang, X., Liu, J. and Li, H., 2017. Surface energy effect on nonlinear free vibration behavior of orthotropic piezoelectric cylindrical nano-shells. *European Journal of Mechanics / A Solids*, 66, pp.423-432.

[23] Lim, C. W., Li, C. and Yu, J. L., 2012. Free torsional vibration of nanotubes based on nonlocal stress theory. *Journal of Sound and Vibration*, *331*, pp.2798-2808.

[24] Li, L. and Hu, Y., 2017. Torsional vibration of bi-directional functionally graded nanotubes based on nonlocal elasticity theory. *Composite Structures*, *172*, pp.242-250.

[25] Murmu, T., Adhikari, S. and Wang, C., 2011. Torsional vibration of carbon nanotube–buckyball systems based on nonlocal elasticity theory. *Physica E: Low-dimensional Systems and Nanostructures*, *43*, pp.1276-1280.

[26] Nazemnezhad, R. and Fahimi, P., 2017. Free torsional vibration of cracked nanobeams incorporating surface energy effects. *Applied Mathematics and Mechanics*, *38*, pp.217-230.

[27] Jena, S.K., Chakraverty, S. and Malikan, M., Tornabene, F., 2021. Stability analysis of single-walled carbon nanotubes embedded in winkler foundation placed in a thermal environment considering the surface effect using a new refined beam theory. *Mechanics Based Design of Structures and Machines*, *49*(4), pp.581-595.

[28] Jena, S.K., Chakraverty, S. and Malikan, M., Tornabene, F., 2020. Effects of surface energy and surface residual stresses on vibro-thermal analysis of chiral, zigzag, and armchair types of SWCNTs using refined beam theory. *Mechanics Based Design of Structures and Machines*, https://doi.org/10.1080/15397734.2020.1754239.

[29] Malikan, M., Krasheninnikov, M. and Eremeyev, V.A., 2020. Torsional stability capacity of a nano-composite shell based on a nonlocal strain gradient shell model under a three-dimensional magnetic field. *International Journal of Engineering Science*, *148*, pp.103210.

[30] Sedighi, H. M. and Malikan, M., 2020. Stress-driven nonlocal elasticity for nonlinear vibration characteristics of carbon/boron-nitride hetero-nanotube subject to magneto-thermal environment. *Physica Scripta*, *95*, pp.055218.

[31] Sedighi, H.M., Malikan, M., Valipour, A. and Żur, K.K., 2020. Nonlocal vibration of carbon/boron-nitride nano-hetero-structure in thermal and magnetic fields by means of nonlinear finite element method. *Journal of Computational Design and Engineering*, *7*, pp.591-602.

[32] Malikan, M. and Eremeyev, V. A., 2020. On the geometrically nonlinear vibration of a piezo-flexomagnetic nanotube. *Mathematical Methods in the Applied Sciences*, https://doi.org/10.1002/mma.6758.

[33] Zarezadeh, E., Hosseini, V. and Hadi, A., 2020. Torsional vibration of functionally graded nano-rod under magnetic field supported by a generalized torsional foundation based on nonlocal elasticity theory. *Mechanics Based Design of Structures and Machines*, 48, pp.480-495.

[34] Noroozi, R., Barati, A., Kazemi, A., Norouzi, S. and Hadi, A., 2020. Torsional vibration analysis of bi-directional FG nano-cone with arbitrary cross-section based on nonlocal strain gradient elasticity. *Advances in Nano Research*, 8, pp.13-24.

[35] Barati, A., Adeli, M. and Hadi, A., 2020. Static torsion of bi-directional functionally graded microtube based on the couple stress theory under magnetic field. *International Journal of Applied Mechanics*, 12, pp.2050021.

[36] Rao, S.S., *Vibration of continuous systems*. Wiley Online Library, (2007).

[37] Gheshlaghi, B. and Hasheminejad, S.M., 2010. Size dependent torsional vibration of nanotubes. *Physica E: Low-dimensional Systems and Nanostructures*, *43*, pp.45-48.

[38] Nazemnezhad, R., Rabiei, M., Shafa'at, P. and Es'haghi, M., 2021. Large amplitude free torsional vibration analysis of size-dependent circular nanobars using elliptic functions. *Structural Engineering and Mechanics, 77,* pp.535-547.

[39] Jamali Shakhlavi, S., Hosseini-Hashemi, S. and Nazemnezhad, R., 2020. Torsional vibrations investigation of nonlinear nonlocal behavior in terms of functionally graded nanotubes. *International Journal of Non-Linear Mechanics*, *124*, pp.103513.

[40] Setoodeh, A.R., Rezaei, M. and Zendehdel Shahri, M.R., 2016. Linear and nonlinear torsional free vibration of functionally graded micro/nano-tubes based on modified couple stress theory. *Applied Mathematics and Mechanics*, *37*, pp.725-740.